THERMAL INFRA-RED BAND CALIBRATION AND LST VALIDATION OF LANDSAT-7 ETM+ INSTRUMENT USING DIFFERENT ATMOSPHERIC PROFILES

Dražen Skoković[1], Jose Antonio Sobrino[1], Juan Carlos Jiménez-Muñoz[1], Gillem Sòria[1], Yves Julien[1]

1. University of Valencia, Global Change Unit - Image Processing Laboratory, Paterna, Spain; drazen.skokovic@uv.es

ABSTRACT

Due to problems in the Thermal Infra-Red Sensor on-board Landsat 8 satellite, thermal data of Landsat 7 recover interest since it is the only source of well calibrated, free and high resolution data. To contribute to the quality of thermal data, a vicarious calibration of the Enhanced Thematic Mapper (ETM+) instrument have been performed during years 2013 to 2015 over two Spanish test sites. These areas (Barrax and Doñana) are included in the framework of the CEOS-Spain project aimed to setting-up experimental zones in Spain for calibration and validation purpose. Different atmospheric profile datasets were used to better characterize the error due to atmospheric correction: i) MODIS atmospheric product MOD07 version 5, ii) MOD07 version 6, and iii) National Center for Environmental Prediction (NCEP) reanalysis data. The calibration results show a constant bias (ETM+ radiance observed minus predicted at sensor radiance) of -0.5 K, with Root Mean Square Errors (RMSE) of 0.7 K.

Land Surface Temperature (LST) was retrieved from the Single-Channel (SC) algorithm as well as through inversion of the Radiative Transfer Equation (RTE). LST retrievals were validated by using in-situ measurements over the different test sites. Depending on atmospheric dataset, validation results for SC algorithm show bias (in-situ LST minus algorithm LST) values between 0 K and 0.7 K and values between 0.4 K and 0.7 K using RTE. RMSE values ranged from 1.4 K to 2 K. For high water vapour content, RTE obtain better accuracy results than the SC algorithm (1.4 K vs. 1.8 K)

INTRODUCTION

In-flight calibration methods, referred to as Vicarious Calibration (VC), are essential to ensure highly consistent and accurate radiometric calibration of Earth Observation (EO) sensors (1). In particular, the need for VC of Thermal Infra-Red (TIR) bands has been recognized since the launch of the Landsat series (2,3,4,5), the only EO platform providing long-term (since 80s) high spatial resolution TIR. Today, two Landsat platforms remain operational: Landsat 7, launched in 1999 and Landsat 8, launched in 2013. The most recent Landsat platform carries on board a TIR sensor (TIRS) that is the first with two TIR bands (band 10 and 11) and spatial resolution of 100 m (6). However, recent calibration and stray light problems in both bands (7) in addition to scene select mirror anomaly (http://landsat.usgs.gov, last date accessed: 02 Jun 2015) decreases precision of TIR data and, consequently, the retrieved of LST. For this reason, Landsat 7 recover interest since it is the only source of well calibrated, free and high resolution data.

The ETM+ instrument, carried by Landsat 7, collects data at 60 m spatial resolution with one band, band 6 (b6), located in TIR region in a window of 10.3 – 12.3 µm. This band has been continuously monitored since 1999. The data obtained during these years allowed the identification of two calibration problems: The first was the observation of constant bias in the data of 3.1 K in the end of year 2000 (5), and the second one was a small gain correction identified in year 2010 with associated bias (at 300 K) of 0.8 K (5). These corrections have contributed to increase the quality of TIR data.

LST is an important parameter that can be obtained from TIR data. The precision in the estimation of LST is a key factor in geo-biophysical studies (8,9) and therefore the accuracy of the algorithms

used in the estimation of the LST must be perform. Specially, two algorithms were used for LST retrieval: SC algorithm developed in (10) and the RTE.

In this paper, in-depth analysis of the TIR band was performed. First, we carried out a VC of TIR data and then a validation of the algorithms proposed to estimate LST. Furthermore, three atmospheric profiles have been evaluated in order to assess atmospheric influence on LST retrieval.

METHODS

1. RADIATIVE TRANSFER EQUATION

VC of TIR band can be performed from both ground-based measurements of radiance or surface temperature (11-12). Since the radiance-based approach requires a field radiometer with similar spectral bands than the sensor to be calibrated, we used a temperature-based approach for the VC of ETM+ band. In this approach, the at-sensor radiance (L_{sen}) is predicted from RTE given by

$$L_{sen} = [\varepsilon B_{Ts} + (1-\varepsilon)L_d]\tau + L_u \quad (1)$$

where ε is the surface emissivity, B_{Ts} is the Planck function for a given LST T_S, and τ, L_u, and L_d are the atmospheric transmissivity, the up-welling atmospheric radiance, and the down-welling atmospheric radiance, respectively. Applying the inverse Planck function, the LST can be estimated as

$$T_S = c_2 \Big/ \lambda \ln\left\{\frac{c_1}{\lambda^5\left[\frac{L_{sen}-L_u-\tau(1-\varepsilon)L_d}{\tau\varepsilon}\right]}+1\right\} \quad (2)$$

where $\boldsymbol{\lambda}$ is the band wavelength and $\boldsymbol{c_1}$ and $\boldsymbol{c_2}$ are the Planck's radiation constants, with values of 1.19104×10^8 W·μm^4·m^2·sr^{-1} and 14387.7 μm·K respectively.

2. SINGLE CHANEL ALGORITHM

The Single-Channel (SC) algorithm retrieves LST using the following general equation:

$$T_S = \frac{T_{sen}^2}{b_\gamma L_{sen}}\left[\frac{1}{\varepsilon}(\Psi_1 L_{sen}+\Psi_2)+\Psi_3\right]+T_{sen}-\frac{T_{sen}^2}{b_\gamma} \quad (3)$$

with T_{sen} the at-sensor brightness temperature, $b_\gamma = c_2/\lambda$ (1277 K for ETM+ band), and Ψ_1, Ψ_2 and Ψ_3 are the so-called atmospheric functions. The practical approach proposed in the SC algorithm consists of the approximation of the atmospheric functions versus the atmospheric water vapour content (w) from a second order polynomial fit:

$$\begin{bmatrix}\psi_1\\ \psi_2\\ \psi_3\end{bmatrix} = \begin{bmatrix}c_{11} & c_{12} & c_{13}\\ c_{21} & c_{22} & c_{23}\\ c_{31} & c_{32} & c_{33}\end{bmatrix}\begin{bmatrix}w^2\\ w\\ 1\end{bmatrix} \quad (4)$$

In the paper, four atmospheric relations between atmospheric functions and water vapour have been analysed: one with atmospheric standard profiles included in MODTRAN (SC_{STD}) and three with the Thermodynamic Initial Guess Retrieval (TIGR) database (SC_{61}, SC_{1761} and SC_{2311}). The numbers indicates the amount of atmospheric profiles included in database. SC (ψ) algorithm presented in eq. 3 and the water vapour approach SC *(w)* have been tested in the paper. More information in (10).

3. TEST SITES AND GROUND DATA

Two Spanish test sites with different natural land cover and climate were considered to collect the in situ data required for the VC and algorithms validation. These test sites include permanent stations for continuous measurements of surface temperature. Three stations are located in the National

Park of Doñana, in South West Spain, near the Atlantic Ocean coast (37ºN, 6.4º W) and another one in the agricultural area of Barrax, located in Albacete, in the centre of Spain (39˚N, 2˚W). Situation and plots of the test sites is shown in figure 1.

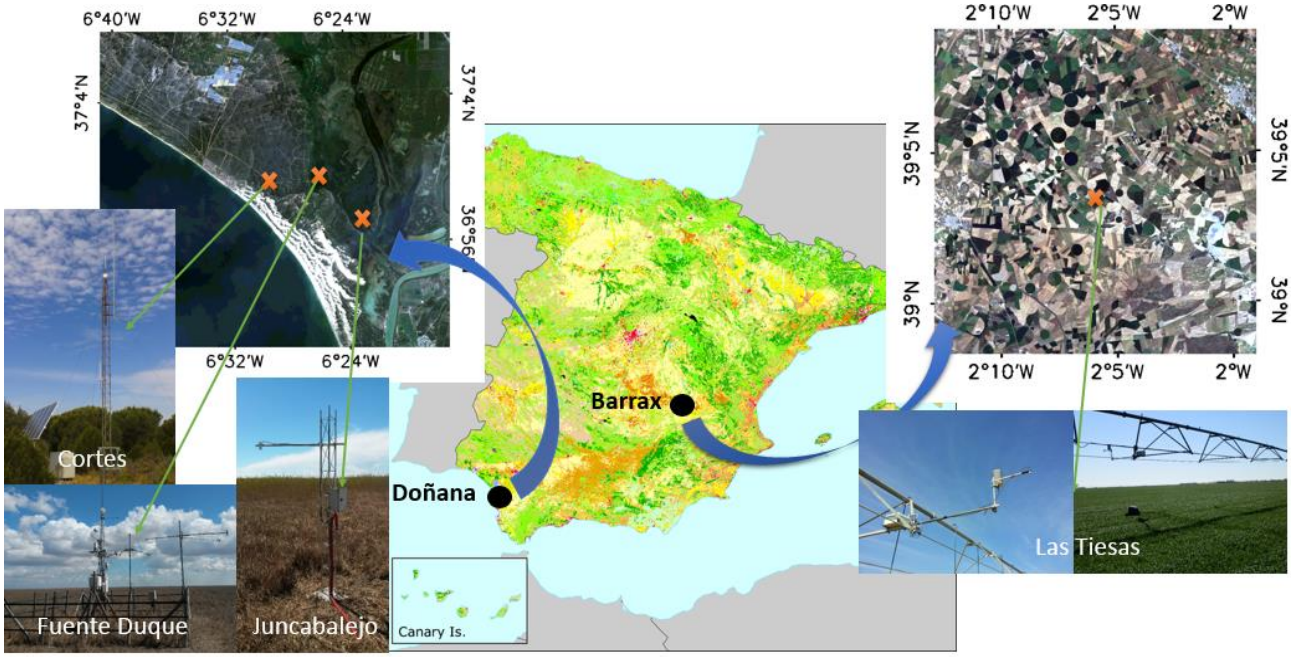

Figure 1: Test sites locations and plots of the fixed stations in the agricultural area of Barrax and in the National Park of Doñana.

Thermal radiance was measured over the test sites using IR120 (Campbell Scientific) and apogee broadband radiometers (8-14 µm). The measurements of the radiometers covers an area of 2 m^2 and this are performed every 5 min. In situ LST were obtained after correction of thermal radiance from ground-based measurements of surface emissivity, and also from measurements of down-welling irradiance using a diffuse reflectance standard plate (Infragold, Labsphere Inc.).

4. ATMOSPHERIC PEROFILES AND LANDSAT 7 IMAGERY DATA

The atmospheric parameters (τ,L_u and L_d) and total column atmospheric water vapor were obtained from three different atmospheric profiles and MODTRAN (version 5) radiative transfer code (13). MODTRAN spectral outputs were finally convoluted with the spectral response functions of ETM+ band 6. Atmospheric profiles used are: i) The MODIS, MOD07 product (14), version 5; ii) MOD07 version 6; iii) Reanalysis data provided by NCEP (15). A direct comparison of the brightness temperature and LST was performed in order to obtain an intercompared accuracy, in kelvin, of the atmospheric profiles.

Forty daytime Landsat 7 scenes were acquired in the period between June 2013 and March 2015 (see table 1). To obtain the radiance value of our test sites, an array of 3x3 pixels centred on the test sites was selected to calculate the mean radiance. Finally, 55 and 30 radiance values have been used for the validation and calibration activities, respectively. For calibration, only the atmospheric water vapour values below 1.5 g/cm^2 were used in order to reduce atmospheric errors. For validation, all the data was used.

Table 1: Number of radiance values obtained from band 6 of ETM+ instrument in our test sites.

Activity	Barrax	Doñana			Total data
	Las Tiesas	Fuente Duque	Juncabalejo	Cortes	
Validation	19	21	4	11	55
Calibration	15	7	2	6	30

RESULTS

1. VICARIOUS CALIBRATION

Predicted at-sensor radiances were compared to radiance values extracted from the ETM+ imagery over the different plots. The results are presented in Figure 2, and the details on the slope (gain), coefficient of determination (R^2), 1-sigma standard deviation (σ) and Root Mean Square Error (RMSE) are given in Table 2.

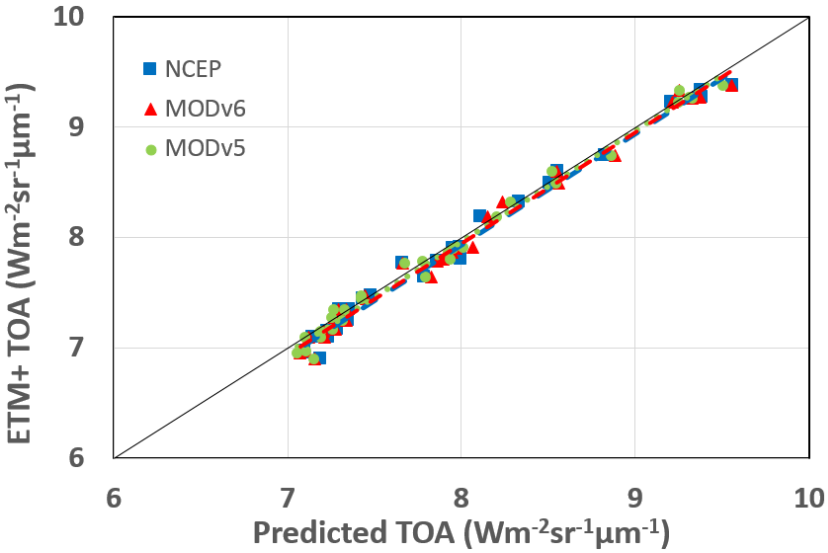

Figure 2: Plot of ETM+ b6 radiance versus the VC-based radiance (predicted). Results are provided for three atmospheric profiles: MOD07 product (version 5 and 6) and the NCEP reanalysis profiles.

Table 2: Results of vicarious calibration between ETM+ b6 values versus obtained from in situ predicted data. The table shows the statics of VC for different atmospheric profiles. Values of bias, σ and RMSE are given in W/m²·sr·µm (K), where σ is the 1 sigma standard deviation.

Atmosphere	Slope	R^2	bias	σ	RMSE
MOD07 v5	0.99±0.02	0.99	-0.044 (-0.4)	0.072 (0.6)	0.084 (0.7)
MOD07 v6	0.99±0.02	0.99	-0.068 (-0.5)	0.081 (0.7)	0.106 (0.8)
NCEP	1.00±0.02	0.99	-0.077 (-0.6)	0.077 (0.6)	0.109 (0.9)

Predicted and b6 derived radiances show a high linear correlation above 1:1 line. Bias and σ are similar in all atmospheric database, with minimal differences (about 0.2 K) and mean values of -0.5 K and 0.7 K, respectively. Bias was calculated as b6 radiance minus predicted (VC) radiance.

2. LST VALIDATION

RTE, SC (ψ) and the SC (w) approximation have been validated with in situ measurements and for the three atmospheric profiles. To obtain the precision depending of the w, three validations have been performed with all data, values of w below 1.5 g/cm² and values of w above 1.5 g/cm². In table 3, bias (as in situ minus algorithm LST), σ and RMSE have been provided for all algorithms and atmospheric profiles.

For all w database, the RMSE with NCEP atmospheric profiles obtain the lowest values for SC (w) approach (0.5 K smaller than MOD07 product). Same results for all SC (w) independently of atmospheric database, except for TIGR1761. This can be explained as 35% of database are artic

Table 3: Results of vicarious calibration between b6 values versus obtained from in situ predicted data. The table shows the statics of VC for different atmospheric profiles. Values of bias, σ and RMSE are given in W/m²·sr·μm (K), where σ is the 1 sigma standard deviation.

Atm. profile	Algorithm	All w			w < 1.5 g/cm²			w > 1.5 g/cm²		
		bias	σ	RMSE	bias	σ	RMSE	bias	σ	RMSE
MOD07 v5	RTE-SC (ψ)	0.4	1.3	1.3	0.4	0.6	0.8	-0.1	1.6	1.6
	SC_{STD}	-0.5	2.0	2.1	-0.4	0.8	0.9	-2.0	2.4	3.1
	SC_{TIGR61}	-0.4	1.8	1.9	-0.2	0.8	0.8	-1.6	2.1	2.7
	$SC_{TIGR1761}$	-0.7	2.2	2.3	-0.3	0.9	0.9	-2.6	2.5	3.7
	$SC_{TIGR2311}$	-0.3	1.9	1.9	0.0	0.8	0.8	-1.3	2.2	2.6
MOD07 v6	RTE-SC (ψ)	0.4	1.3	1.4	0.6	0.7	0.9	-0.2	1.6	1.6
	SC_{STD}	-0.5	1.9	1.9	-0.2	0.8	0.8	-1.5	2.2	2.7
	SC_{TIGR61}	-0.3	1.7	1.8	-0.1	0.8	0.8	-1.4	2.1	2.5
	$SC_{TIGR1761}$	-0.4	2.1	2.1	-0.2	0.8	0.8	-2.3	2.4	3.3
	$SC_{TIGR2311}$	-0.2	1.7	1.8	0.1	0.8	0.8	-1.0	2.1	2.3
NCEP	RTE-SC (ψ)	0.7	1.2	1.3	0.7	0.8	1.1	0.6	1.4	1.6
	SC_{STD}	-0.4	1.4	1.5	-0.3	0.8	0.9	-0.9	1.8	2.0
	SC_{TIGR61}	-0.2	1.4	1.4	-0.2	0.8	0.9	-0.8	1.7	1.9
	$SC_{TIGR1761}$	-0.5	1.6	1.7	-0.3	0.9	0.9	-1.5	1.9	2.4
	$SC_{TIGR2311}$	0.0	1.4	1.4	0.1	0.8	0.8	-0.4	1.7	1.8

profiles, higher than other database. RTE and SC (ψ) results are similar independently of atmospheric database. No differences have been found between algorithms with w below 1.5 g/cm², but for high w, differences are notable. σ turns higher and bias turns more negative (except for RTE and SC (ψ) with NCEP profile that is equal as low w). For SC (w), there are significant differences between atmospheric profiles with best performance for NCEP database.

CONCLUSIONS

Due to problems of Landsat 8 TIRS, Landsat 7 ETM+ instrument recover his interest as the only source of well calibrated, free and high resolution data. For this reason, a VC and validation of LST algorithms with different atmospheric profiles was performed in order to find the accuracy way to estimate LST.

According to the results obtained in the VC, a bias for the thermal band is still observed (-0.5 K, prediction of LST 0.5 K too low), but due to σ obtained in the VC (0.7 K), the results should be confirmed in an independent study.

RTE, SC (ψ) and SC (w) obtain the same results with low atmospheric water vapour content. All of them are recommendable in the estimation of LST.

In high atmospheric water vapour content, SC (w) retrieves the best precision with NCEP profiles, around 0.5-1 K lower than MOD07 product. RTE and SC (ψ) obtain similar RMSE results but the bias turns negative for MOD07 product and for all SC (w) datasets analysed. The LST is overestimated, except for RTE and SC (ψ) obtained with NCEP profiles.

In conclusion, RTE and SC (ψ) offers the best way to estimate the LST. If the only input available is the water vapour content, it is recommended the use of the $SC_{TIGR2311}$ database as it demonstrated best performance.

ACKNOWLEDGEMENTS

We acknowledge funding from Ministerio de Economía y Competitividad [EODIX, project AYA2008-0595-C04-01; CEOS-Spain, project AYA2011-29334-C02-01], and the FPI grant.

REFERENCES

1 Slater P.N, Biggar S.F, Thome K.J, Gellman D.I. & Spyak P.R, 1996. Vicarious radiometric calibrations of EOS sensors. Journal of Atmospheric and Oceanic Technology, vol. 13, pp. 349-359

2 Schott J. R, Barsi J. A, Nordgren B. L, Raqueno N. G & de Alwis D, 2001. Calibration of Landsat thermal data and application to water resource studies. Remote Sens. Environ., vol. 78, no. 1/2, pp. 108–117

3 Barsi J.A, Schott J.R, Palluconi F.D, Helder D.L, Hook S.J, Markham B.L, Chander G & O'Donnell E.M, 2003. Landsat TM and ETM+ thermal band calibration. Canadian Journal of Remote Sensing, vol.29, no.2, pp. 141–153

4 Coll C, Galve J. M, Sánchez J. M & Caselles V, 2010. Validation of Landsat-7/ETM+ Thermal-Band Calibration and Atmospheric Correction With Ground-Based Measurements. IEEE Trans. Geosci. Remote Sens., vol. 48, no. 1, pp. 547–555

5 Schott R, Hook S. J, Barsi J. A, Markham B. L, Miller J, Padula F. P & Raqueno N. G, 2012. Thermal Infrared Radiometric Calibration of the Entire Landsat 4, 5, and 7 Archive (1982-2010). Remote Sens. Environ., vol. 122, pp. 41–49

6 Irons J. R, Dwyer J. L & Barsi J. A, 2012. The next Landsat satellite: The Landsat Data Continuity Mission. Remote Sens. Environ., vol. 122, pp. 11–21

7 Barsi J. A, Schott J. R, Hook S. J, Raqueno N. G, Markham B. L & Radocinski R. G, 2014. Landsat-8 Thermal Infrared Sensor (TIRS) Vicarious Radiometric Calibration. Remote Sens., 6, 11607-11626.

8 Kalma, J.D, McVicar T.R & McCabe M.F, 2008. Estimating Land Surface Evaporation: A Review of Methods Using Remotely Sensed Surface Temperature Data. Surveys in Geophysics, 29(4-5), 421-469.

9 Kustas W & Anderson M, 2009. Advances in thermal infrared remote sensing for land surface modeling. Agricultural and Forest Meteorology, 149(12), 2071-2081.

10 Jiménez-Muñoz J. C, Cristóbal J, Sobrino J. A, Sòria G, Ninyerola M & Pons X. 2009. Revision of the Single-Channel Algorithm for Land Surface Temperature Retrieval From Landsat Thermal-Infrared Data. IEEE Transactions on Geoscience and Remote Sensing, 47(1), 339-349.

11 Thome K. J, Schiller S, Conel J. E, Arai K & Tsuchida S, 1998. Results of the 1996 Earth Observing System vicarious calibration joint campaign at Lunar Lake Playa, Nevada (USA).Metrologia, vol.35, pp.631-638.

12 Toonoka H, Palluconi F.D, Hook S.J & Matsunaga T, 2005. Vicarious calibration of ASTER thermal infrared bands. IEEE Transactions on Geoscience and Remote Sensing, vol. 432, pp. 1113–1126.

13 Jiménez-Muñoz J. C, Sobrino J. A, Mattar C & Franch B, 2010. Atmospheric correction of optical imagery from MODIS and Reanalysis atmospheric products. Remote Sensing of Environment, vol.114, pp. 2195–2210.

14 Sobrino J. A, Jiménez-Muñoz J. C, Mattar C. & Sòria G, 2014. Evaluation of Terra/MODIS atmospheric profiles product (MOD07) over the Iberian Peninsula: a comparison with radiosonde stations. International Journal of Digital Earth, DOI:10.1080/17538947.2014.936973

15 Barsi J. A, Schott J. R, Palluconi F. D. & Hook S. J, 2005. Validation of a web-based atmospheric correction tool for single thermal band instruments," Proc. SPIE, vol. 5882, pp. 588 20E.1–588 20E.7. DOI: 10.1117/12.619990